Arrhythmogenic Ca^{2+} release from cardiac myofilaments

Henk E.D.J. ter Keurs[a,*], Yuji Wakayama[b], Masahito Miura[b],
Tsuyoshi Shinozaki[b], Bruno D. Stuyvers[a], Penelope A. Boyden[c],
Amir Landesberg[d]

[a]*Departments of Medicine, Physiology and Biophysics; University of Calgary Health Science Centre,
3330 Hospital Drive N.W. Calgary, Alta., Canada T2N4N1*
[b]*First Department of Internal Medicine Tohoku University, School of Medicine, Sendai, Japan*
[c]*Department of Pharmacology, Center for Molecular Therapeutics, Columbia University, NY, USA*
[d]*Faculty of Biomedical Engineering, Technion -Israel Institute of Technology, Haifa, Israel*

Available online 8 August 2005

Abstract

We investigated the initiation of Ca^{2+} waves underlying triggered propagated contractions (TPCs) occurring in rat cardiac trabeculae under conditions that simulate the functional non-uniformity caused by mechanical or ischemic local damage of the myocardium. A mechanical discontinuity along the trabeculae was created by exposing the preparation to a small constant flow jet of solution with a composition that reduces excitation–contraction coupling in myocytes within that segment. Force was measured and sarcomere length as well as $[Ca^{2+}]_i$ were measured regionally. When the jet-contained Caffeine, BDM or Low-$[Ca^{2+}]$, muscle-twitch force decreased and the sarcomeres in the exposed segment were stretched by shortening of the normal regions outside the jet. During relaxation the sarcomeres in the exposed segment shortened rapidly. Short trains of stimulation at 2.5 Hz reproducibly caused Ca^{2+}-waves to rise from the borders exposed to the jet. Ca^{2+}-waves started during force relaxation of the last stimulated twitch and propagated into segments both inside and outside of the jet. Arrhythmias, in the form of non-driven rhythmic activity, were triggered when the amplitude of the Ca^{2+}-wave increased by raising $[Ca^{2+}]_o$. The arrhythmias disappeared when the muscle uniformity was restored by turning the jet off. We have used the four state model of the cardiac cross bridge (Xb) with feedback of force development to Ca^{2+} binding by Troponin-C (TnC) and observed that the force–Ca^{2+} relationship as well as the force–sarcomere length relationship and the time course of the force and Ca^{2+} transients in cardiac muscle can be reproduced faithfully by a single effect of force on deformation of the $TnC \cdot Ca$ complex and thereby on the dissociation

*Corresponding author. Tel.: +403 220 4521.
E-mail address:* terkeurs@ucalgary.ca (H.E.D.J. ter Keurs).

rate of Ca^{2+}. Importantly, this feedback predicts that rapid decline of force in the activated sarcomere causes release of Ca^{2+} from $TnC.Ca^{2+}$, which is sufficient to initiate arrhythmogenic Ca^{2+} release from the sarcoplasmic reticulum. These results show that non-uniform contraction can cause Ca^{2+}-waves underlying TPCs, and suggest that Ca^{2+} dissociated from myofilaments plays an important role in the initiation of arrhythmogenic Ca^{2+}-waves.

1. Introduction

Cardiac disease leads invariably to non-uniformity of myocardium. The role of electrical non-uniformity of the myocardium in re-entry arrhythmias is well established (Spooner and Rosen, 2001). It is less well known to what extent non-uniform myocardial stress and strain distributions and non-uniform excitation–contraction coupling may play a role in the initiation of extra-systoles that start arrhythmias. It is well known that tens of moles (per litre cell volume) of Ca^{2+} shuttle during the cardiac cycle between the sarcoplasmic reticulum (SR) and the cytosol where Troponin-C (TnC) is the dominant ligand. Hence, it is conceivable that non-uniformity of myocardium may lead to extra-systoles by several mechanisms including both abnormal SR-Ca^{2+} transport following damage and abnormal mechanical events in non-uniform myocardium, which cause dissociation of Ca^{2+} from TnC.

It has been shown that "spontaneous" SR-Ca^{2+} release causes both transient inward currents and arrhythmogenic delayed after-depolarizations (DADs) as well as aftercontractions (Ferrier, 1976; Kass et al., 1978). A sufficiently large SR-Ca^{2+} load in cells at the rim of a damaged region could create an unstable state where spontaneous SR-Ca^{2+} release may become so large that the resulting transient inward current depolarizes the cells enough to trigger a new action potential, which perpetuates itself as a triggered arrhythmia (Cranefield, 1977).

Alternatively, events that result from the tug-of-war between normal myocardium and weak cells in the ischemic zone could trigger the Ca^{2+} release and lead to arrhythmias. This tug of war may play a role in Ca^{2+} release, triggered in damaged regions of isolated rat ventricular and human atrial trabeculae, resulting in Ca^{2+} release that appears to be initiated after stretch of the damaged region during the regular twitch and propagates into neighboring myocardium by the combination of Ca^{2+} diffusion and Ca^{2+}-induced SR-Ca^{2+} release. The elevation of $[Ca^{2+}]_i$, which accompanies this process (Fig. 1) causes a propagating contraction (TPC; Fig. 1) (Daniels and ter Keurs, 1990; Mulder et al., 1989)and may depolarize the cell beyond the threshold for action potential generation (Daniels et al., 1991b). This propagating SR-Ca^{2+} release may, therefore, serve as the mechanism that couples regional damage with the initiation of extra-systoles and consequent arrhythmias in the adjacent myocardium (Daniels and ter Keurs, 1990; Mulder et al., 1989).

It is clear that damage of a cardiac cell causes loss of integrity of the cell membrane and allows Ca^{2+} entry into damaged cells and their neighbors, which in its turn will induce SR-Ca^{2+} overload and cause spontaneous microscopic Ca^{2+} release in the latter cells (Mulder et al., 1989). The spontaneous Ca^{2+} release increases resting force and decreases force of the next twitch of
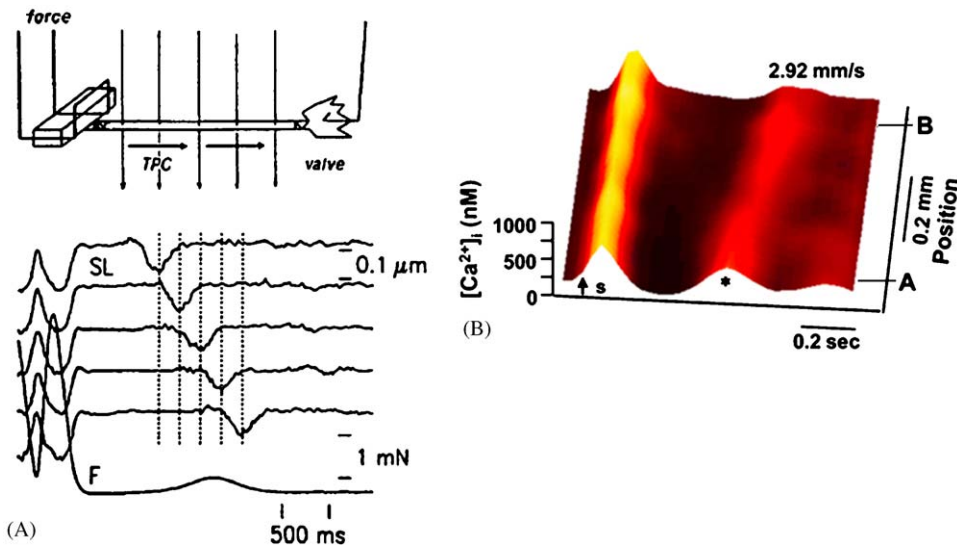
Fig. 1. Panel A: Sarcomere length (SL) recordings at five different sites (each 300 μm apart) along a 2.94 mm long trabecula during a TPC with a propagation velocity of 1.4 mm/s. The interval between peak sarcomere shortening due to the TPC (vertical dashed lines) was constant from site to site, indicating that propagation velocity remained constant along the preparation. F = force. $[Ca^{2+}]_o$ 1.0 mM, temperature 21 °C. Initial sarcomere length varied less than 0.05 μm between the sites of measurement. Modified from (Daniels, 1991; ter Keurs et al., 1998). Panel B: Fig. 6. The Ca^{2+} transients as a function of distance along the preparation at different times. The propagating nature of the Ca^{2+} wave is evident from the figures. Modified from (Miura et al., 1998).

these cells (Kort and Lakatta, 1984; Stern et al., 1983), which sets the scene for a tug-of-war where weakened myocytes are stretched by normal myocytes to which they are linked. The observation that the TPCs always start shortly after the rapid shortening of the damaged areas during the relaxation phase (Daniels et al., 1991b; Mulder et al., 1989) suggests that it is in fact the shortening and force decrease during relaxation that initiates a TPC. In order to understand this phenomenon, we have proposed the existence of reverse excitation–contraction coupling (RECC) (ter Keurs et al., 1998) based on the classical concept of ECC (Fig. 2). The observation (Allen and Kentish, 1985,1988a; Allen and Kurihara, 1982; Backx et al., 1995; Housmans et al., 1983)that rapid shortening and force decline of a contracting muscle causes a *surge of Ca^{2+} release* from the myofilaments provides a candidate mechanism for initiation of TPCs (Daniels and ter Keurs, 1990) (Fig. 2, middle panel). Ca^{2+} that dissociates from the contractile filaments due to the quick release of the damaged areas during relaxation could initiate a wave of Ca^{2+} release if at that time the SR has recovered sufficiently (Banijamali et al., 1991)to allow Ca^{2+}-induced Ca^{2+} release (CICR) to amplify the initial *Ca^{2+} surge* in the damaged region and/or the border zone (Fig. 2, middle panel). The propagating Ca^{2+} transient, in turn, will activate arrhythmogenic Ca^{2+}-dependent depolarizing currents (Fig. 2, right-hand panel) (Daniels et al., 1991a; Kass et al., 1978). The observation that neither initiation of TPCs nor their propagation is affected by Gd^{3+} ions suggests that stretch activated channels play little or no role in the initiation or propagation TPCs (Zhang and ter Keurs, 1994).
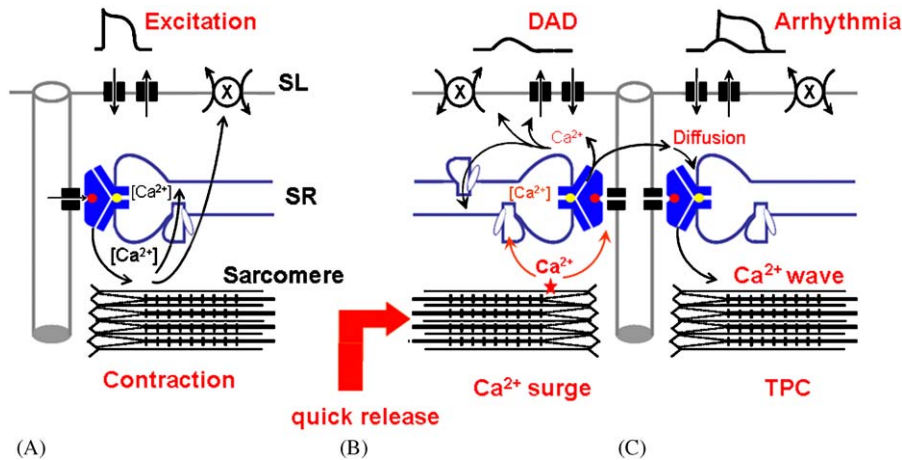
Fig. 2. Excitation–contraction coupling system in the cardiac cell, as well as reverse excitation contraction coupling during TPCs. (A) The events during the twitch: During the action potential a transient Ca^{2+} influx enters the cells followed by a maintained component of the slow inward current. Ca^{2+} entry does not lead directly to force development as the Ca^{2+} that enters is rapidly bound to binding sites on the SR. The rapid influx of Ca^{2+} via the T-tubuliraises $[Ca^{2+}]_i$ in the narrow gap between DHPR and RyR and induces release of Ca^{2+} from the SR, by triggering opening of Ca^{2+} channels in the terminal cisternae, thus activating the contractile filaments to contract. Rapid relaxation follows because the cytosolic Ca^{2+} is sequestered rapidly by the SR and partly extruded through the cell membrane by the Na^+/Ca^{2+} exchanger and by the low capacity high affinity Ca^{2+} pump. This process loads the SR. Na^+/Ca^{2+} exchange is electrogenic so that Ca^{2+} extrusion through the exchanger leads to a depolarizing current. (B) The postulated events in non-uniform muscle during triggering of the TPC. Non-uniform muscle contains weak segments which are stretched by strong segments during the twitch. During rapid relaxation the relatively weak segment rapidly shortens owing to relaxation of stronger myocardium. This quick release of the weak sarcomeres leads to dissociation of Ca^{2+} from the contractile filaments during the relaxation phase. Two mechanisms may cause SR-Ca^{2+} release: (i) the rise in [Ca] from TnC release stimulates the SR pump of closely apposed SR longitudinal element leading to an increase rise in SR luminal $[Ca^{2+}]$ which causes Ca^{2+} release via the RyR (It is established that luminal [Ca] influences RyR Po); (ii) Ca^{2+} from the Ca^{2+} surge entering into the small DHPR-RyR gap may be sufficient to initiate SR-Ca^{2+} release. The SR is enough recovered to respond to the increase in $[Ca^{2+}]_i$ by Ca^{2+}-induced Ca^{2+} release. The resultant elevation of $[Ca^{2+}]_i$ causes diffusion of Ca^{2+} to adjacent sarcomeres. (B) and (C) show that arrival of diffusing Ca^{2+} after release in the damaged region leads to Ca^{2+} release by the SR in the adjacent sarcomeres by similar mechanisms ((i) and (ii)). Ca^{2+} diffuses again the next sarcomere, while causing a local contraction as well as an arrhythmogenic delayed after-depolarization (DAD) due to electrogenic Na^+/Ca^{2+} exchange and activation of Ca^{2+} sensitive non-selective channels in the sarcolemma. Diffusion of Ca^{2+} along its gradient maintains the propagation of the TPC.

A detailed study of the role of strong and weak muscle regions of damaged muscle in the initiation of arrhythmogenic Ca^{2+}-waves is hampered by the difficulty in controlling the extent and severity of damage, and as such neither SL nor $[Ca^{2+}]_i$ can be measured reliably. Here, we show early experimental results using a novel model of controlled non-uniformity in rat trabeculae. Using this approach, we show that controlled initiation of propagating Ca^{2+}-waves underlying TPCs can trigger non-driven repetitive regular spontaneous contractions in cardiac muscle, i.e. arrhythmogenicity of non-uniform muscle. Then, we show that a cardiac XB model

(Landesberg and Sideman, 1994a, b), based on the effect of feedback of XB-force to binding of Ca^{2+} to TnC suggests that initiation of arrhythmogenic Ca^{2+}-waves can be explained by non-uniformity in ECC leading to a Ca^{2+}-surge from TnC as a result of rapid force decline in the weak regions of non-uniform muscle during relaxation of stronger regions. In conclusion, we propose that TnC is the source of a "funny" Ca^{2+} surge that leads to arrhythmogenic Ca^{2+} waves in mechanically non-uniform cardiac muscle.

2. Methods

2.1. Measurements of force, SL and $[Ca^{2+}]_i$ in rat trabeculae

Trabeculae were dissected from the right ventricle of Lewis Brown Norway rats and mounted between a motor arm and force (F) transducer in a bath perfused by HEPES solution on an inverted microscope. Sarcomere length (SL) was measured by laser diffraction techniques (ter Keurs et al., 1980b). Measurement of $[Ca^{2+}]_i$ has been described previously (Backx and ter Keurs, 1993; Miura et al., 1998, 1999; Wakayama et al., 2001). Briefly, Fura-2 salt was microinjected iontophoretically into the trabecula (Backx and ter Keurs, 1993). Excitation light of 340, 360 or 380 nm was used and fluorescence was collected using an image intensified CCD camera (IIC) to assess local $[Ca^{2+}]_i$ (Backx and ter Keurs, 1993). Variations in $[Ca^{2+}]_i$ along the trabeculae were calculated from the calibrated ratio of $F_{360}//F_{380}$.

### 2.2. Reduction of local contraction and induction of Ca^{2+}-waves

To produce non-uniform ECC, a restricted region was exposed to a small "jet" of solution (≈ 0.06 ml/min) that had been directed perpendicularly to a small muscle segment (300 μm; Fig. 3) using a syringe pump connected to a glass pipette (≈ 100 μm diameter; Fig. 3A) (Wakayama et al., in review). The jet solution contained standard HEPES solution as well as either: (1) caffeine (CF; 5 mmol/L) to deplete SR of Ca^{2+} through opening of the SR-Ca^{2+} release channels (Bers, 2001; Konishi et al., 1984; Sitsapesan and Williams, 1990; Young et al., 2001); (2) 2,3-butanedione monoxime (BDM; 20 mmol/L) to suppress myosin ATPase and, thus, activation of XBs (Backx et al., 1994; Herrmann et al., 1992; Sellin and McArdle, 1994) while reducing the SR-Ca^{2+} content modestly or (3) Low $[Ca^{2+}]$ (Low-$[Ca^{2+}]_{jet}$; 0.2 mmol/L) to reduce Ca^{2+} availability for ECC (Bers, 2001). The Ca^{2+}-concentration in the jet ($[Ca^{2+}]_{jet}$) was usually identical to the bath solution ($[Ca^{2+}]_o$), except for Low-$[Ca^{2+}]_{jet}$ solution or unless mentioned otherwise. During exposure to the jet solutions, Ca^{2+}-waves underlying TPCs were induced by stimulation of the muscle at 2.5 Hz for 7.5 s repeated every 15 s at $[Ca^{2+}]_o$ of 2–3 mmol/L at 24 °C (Daniels et al., 1991b). Measurement of $[Ca^{2+}]_i$ commenced within 10 min, as soon as the amplitude of stimulated twitches, TPCs and underlying Ca^{2+}-waves were constant.
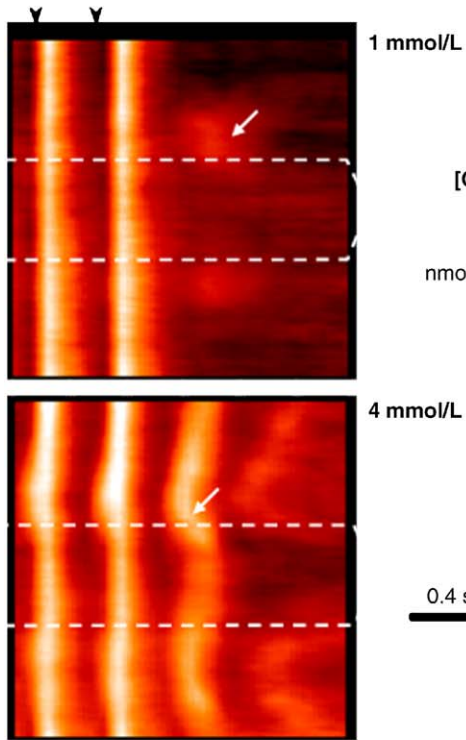
2.3. Data analysis

Data were expressed as mean$\pm$SEM. Statistical analysis was performed using ANOVA followed by a Post hoc test. Differences were considered significant when $p < 0.05$.
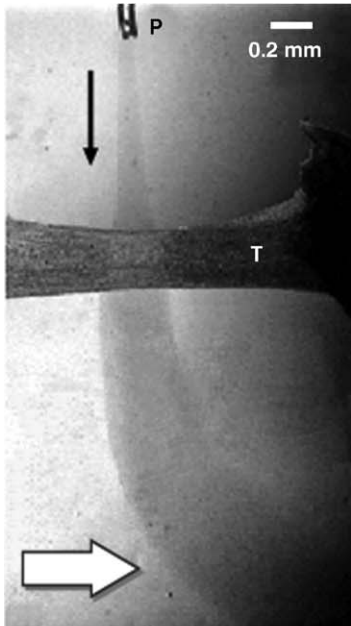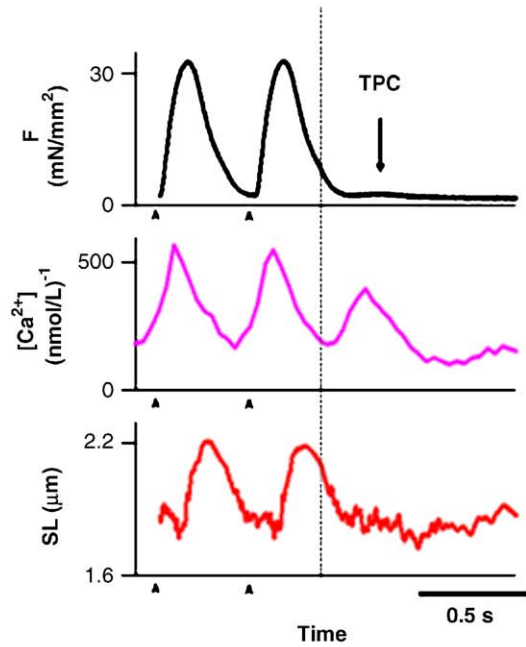
(A)
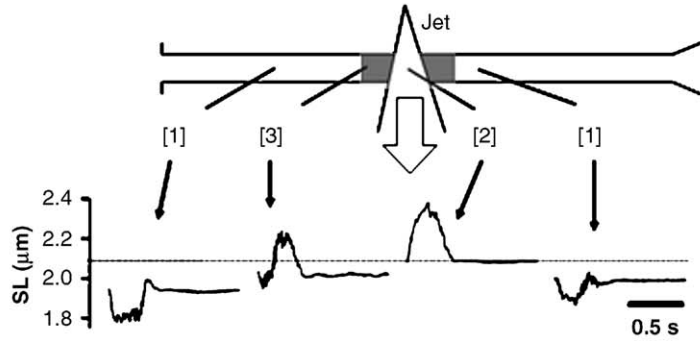
(B)

(C)

(D)

2.4. Model simulations

We simulated experimentally observed Ca^{2+} transients and twitch kinetics to gain insight into the parameters of the Ca^{2+} release and removal processes that dictate their time course. The model was simplified after the model of Michailova et al. (2002) and assumes release, ligand binding, uptake and diffusion of Ca^{2+}. Opening of Ca^{2+} channels was operator initiated. We assumed a pulse-shaped Ca^{2+} release flux (R) with an exponential rise and fall:

$$R = a(1 - e^{-(t-t_s/\tau_{on})})e^{-(t-t_s/\tau_{off})}.$$

Released Ca^{2+} binds to ATP, Fluo-4 and TnC according to the reaction of the general form:

$$Ca^{2+} + Ligand \underset{K_-^L}{\overset{K_+^L}{\rightleftharpoons}} Ca - Ligand$$
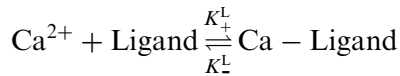
with ligand concentrations (Ligand) and rate constants (K_+^L, K_-^L) as given by Csernoch et al. (2004) adjusted to 26 °C assuming a Q_{10} of 2. We assumed that the $[Mg^{2+}]_i$ was constant (1 mM) and that ATP only binds Ca^{2+} and Mg^{2+}. The flux of Ca^{2+} elimination (U) was assumed to follow Hill kinetics. We used the parameters for Ca^{2+} uptake by the SR measured for Cardiac myocytes in the laboratory (Davidoff et al., 2004):

$$U = \frac{U_{MAX} \cdot [Ca]_N^{Hill}}{EC_{U_{50}}^{Hill} + [Ca]_N^{Hill}}.$$

The Hill coefficient (Hill = 2.2) was assumed to be constant. EC_{U50} and U_{MAX} were fitted to the experimental data. $[Ca \cdot TnC]$, $[Ca \cdot Fluo4]$ were calculated from:

$$\frac{d[Ca]}{dt} = R - U - k_+^{ATP}([ATP] - [Ca.ATP])[Ca]$$
$$+ k_-^{ATP}[Ca.ATP] - k_+^{TnC}([TnC] - [Ca.TnC])[Ca]$$

Fig. 3. Non-uniform cardiac muscle and $[Ca^{2+}]_i$. (A) A micrograph of a trabecula in which is superfused with HEPES solution (white arrow). A micropipette provides a jet of solution (dark grey) oriented perpendicular to the long axis of the muscle (black arrow). The composition of the jet is chosen so as to modify EC coupling in the region of the muscle exposed to the jet (B) SL changes in three regions of the muscle during the twitch during exposure to a jet containing BDM (20 mmol/L)l. Segment [1] is not affected by the jet ; segment [2] is in the center of the jet; segments [3] form the border zone between region [1] and [2]. Normal contraction in segments [1] is accompanied by stretch in [2], while segment [3] shows initial contraction followed by later stretch during the twitch. (C) The $[Ca^{2+}]_i$ (in color code; see calibration bar) along the muscle (ordinate) as a function of time (abscissa) during and after two electrically driven contractions. The region subjected to the jet is delineated by the dashed lines. The panel shows the initiating events of Ca^{2+}-waves induced by local BDM (20 mmol/L) exposure. At Low $[Ca^{2+}]$ in the bath (1 mmol/L, top panel) only a local Ca^{2+}-surge (starting 360 ms) after stimulation is observed. Increasing $[Ca^{2+}]_o$ to 4 mmol/L (bottom panel) led to the initiation of bi-directional Ca^{2+}-waves, which propagate into the segment inside the jet and into the normal muscle. Both amplitude of the initial and propagating transient as well as propagation velocity increased with increase of $[Ca^{2+}]_o$, while the latency of onset of the Ca^{2+}-transient decreased (300 ms). Arrows indicate initiation sites of propagating waves. The occurrence of $[Ca^{2+}]_i$ transients in the border zone prior to the stimulated $[Ca^{2+}]_i$ transient is visible at higher $[Ca^{2+}]_o$. (D) The time course of force $[Ca^{2+}]_i$ and SL during the twitch in the border zone [3]. It is clear that the $[Ca^{2+}]_i$ transient of the triggered propagated contraction (TPC) is initiated following the quick release of force and SL in this region.($[Ca^{2+}]_o$ in the bath : 2.0 mmol/L).

$$+ k_-^{TnC}[Ca.TnC] - k_+^{Fluo4}([Fluo4] - [Ca.Fluo4])[Ca]$$
$$+ k_-^{Fluo4}[Ca.Fluo4]$$

F, actin strain and Ca^{2+} binding on TnC:

We assumed that $[Ca \cdot TnC]$ enables XB formation and force development, which was calculated from

$$d[XB]/dt = ([TnCa]/[TnC]_{total})f[XB_{free}] - g[XB_{att}],$$

where f and g are the rates of XB attachment and detachment, respectively. We assumed that force by the XBs is proportional to the unitary XB force (2–6 pN) and is transmitted by actin; actin was assumed to exhibit a stiffness constant $= \kappa$, resulting in an exponential strain (ε) in response to force:

$$\varepsilon = e^{\wedge}(F \bullet \kappa).$$

It is known that Ca^{2+} binding to TnC is diffusion limited (Michailova et al., 2002). Hence we chose to create a feedback of force to Ca^{2+}–TnC kinetics by assuming that deformation of actin is accompanied by a structural change of TnC which reduces the rate of dissociation of bound Ca^{2+}.

$$k_- = k'_-/\varepsilon,$$

where k'_- is the rate of dissociation of Ca^{2+} from TnC on unstrained actin.

The cytosolic $[Ca^{2+}]_i$ was assumed to be 70 nM (Stuyvers et al., 1997) and the calculations were started with the buffers in equilibrium. For simplification we have neither incorporated other ligands nor other buffering systems known to exist in cardiac myocytes (Bers, 2001; Fabiato, 1983). The calculations were performed with an integration interval of 1 μs. Rise times of $[Ca^{2+}]_i$ transients were simulated by fitting the rate constants of Ca^{2+} channel opening and closing, their open time (Δt), and R to the experimentally observed rising phase of the Ca^{2+} transient. The decline of a Ca^{2+} transient was simulated by fitting U_{max} and EC_{U50} to the observed decline of the transients in the absence of F (Ishide et al., 1992).

2.5. F–pCa relationships: time course of the twitch and effects of quick releases

For the steady state F–pCa relationship we assumed Hill behavior, while the interaction between F and the K_D of $Ca \cdot TnC$ was strain dependent:

$$F = F_{max}[Ca^{2+}]_i/(K_D + [Ca^{2+}]_i) \text{ and } K_D = k_-/k_+ = k'_-/\varepsilon$$

F_{max} at saturating $[Ca^{2+}]_i$ is a function of acto-myosin overlap, which depends on the geometry of the sarcomere (ter Keurs et al., 2000). The feedback coefficient ε depends on the stiffness coefficient κ of actin and was identical for simulations of each of the relationships.

3. Experimental results

3.1. Experimental non-uniformity and sarcomere mechanics

Fig. 3 shows the experimental model of non-uniformity in a cardiac trabecula using a jet of fluid that reached only a small segment of the muscle while the remainder was exposed to the main

solution that perfused the muscle bath. The jet reached one short muscle segment ($\sim$300 μm). The fluid flow from the pipette using a solution with composition similar to the HEPES solution in the bath had no effect on F or SL by itself. Although we have studied the effects of BDM (Fig. 3), Caffeine and Low-[Ca^{2+}] in the jet applied from aside to the muscle, we will focus of the effects of BDM here.

When a jet containing either BDM (Fig. 3A) or Caffeine or Low-[Ca^{2+}] (data not shown) was applied to the stimulated trabeculae, sarcomere stretch replaced rapidly the normal active shortening of the sarcomeres in the exposed segment, while peak force (F/F_{max}) decreased by 10–35% depending on the contents of the jet solution. The jet solution affected resting SL little in Caffeine or Low-[Ca^{2+}] (data not shown), but usually caused some lengthening in the jet with BDM (Fig. 3A). All effects were rapidly reversible. Sarcomere dynamics along muscles exposed to a jet revealed three distinct regions during the stimulated twitch (Fig. 3B): (i) a region located $>$200 μm from the jet where sarcomeres exhibited typical shortening; (ii) the segment exposed to the jet where sarcomeres were stretched; (iii) in a 'Border Zone' (BZ) between these two segments, sarcomeres shortened early during the twitch and, then, were stretched (Fig. 3B). Sarcomere stretch in the BZ was less than in the jet-exposed segment. The BZ extended 1–2 cell lengths beyond the jet-exposed region. Similar changes in regional sarcomere dynamics were observed in Caffeine and Low-[Ca^{2+}]$_{jet}$ experiments.

3.2. Non-uniformity and [Ca^{2+}]$_i$ transient

In contrast to the similarity of the effects of the various jet solutions on sarcomere dynamics, jets of Caffeine, BDM or Low-[Ca^{2+}]$_o$ solution had distinct effects on [Ca^{2+}]$_i$. Robust electrically driven [Ca^{2+}]$_i$-transients occurred in the regions outside the jet independent of the composition of the jet solution (Fig. 3C). As expected, both the Caffeine-jet and Low-[Ca^{2+}]$_{jet}$ decreased the peak of the stimulated [Ca^{2+}]$_i$-transient; this contrasted the effect of BDM, which decreased the [Ca^{2+}]$_i$-transient only slightly (Fig. 3C). The effect of caffeine to increase diastolic [Ca^{2+}]$_i$ in the jet region was opposite to that of Low-[Ca^{2+}]$_{jet}$ and BDM which both decreased diastolic [Ca^{2+}]$_i$. The [Ca^{2+}]$_i$- changes were smaller in the BZ, consistent with a gradient between regions due to mixing of the contents of the jet with the main solution in the bath. Ca^{2+}-waves started systematically in the BZ after the decline of the last stimulated Ca^{2+}-transient (Fig. 3D). These waves propagated into the regions outside and—in the cases of BDM and Low-[Ca^{2+}]$_{jet}$—inside the jet-exposed region. Fig. 3C (BDM jet) clearly shows two initiation sites of four Ca^{2+}-waves in the BZ and symmetric propagation into regions outside and inside the jet.

3.3. Initiation of Ca^{2+}-waves

Fig. 3 shows initiation of Ca^{2+}-waves in the BZ of a BDM exposed trabeculae. All muscles responded reproducibly to increasing [Ca^{2+}]$_o$ at [Ca^{2+}]$_o$ = 1 mmol/L (Fig. 3C A top), only a localized transient in [Ca^{2+}]$_i$ ($\approx$300 nmol/L)—denoted as 'Ca^{2+}-surge'(see arrow)—occurred along $\sim$100–150 μm of the BZs without apparent propagation of Ca^{2+} waves. The Ca^{2+}-surge took place $\sim$325 ms after the stimulus, during the relaxation phase of the twitch, when Force had declined by 70–80% (Fig. 3D). Increasing [Ca^{2+}]$_o$ led to a decrease of the latency and an increase of the Ca^{2+}-surge (Fig. 3C-bottom) and led to development of bi-directional propagating

Ca^{2+}-waves. The initial Ca^{2+}-surge always occurred in the BZs late during relaxation of the last stimulated Ca^{2+}-transient. Increasing $[Ca^{2+}]_o$ further also increased the velocity of propagation of the Ca^{2+}-waves.

Similar observations were made in Low-$[Ca^{2+}]_{jet}$ exposed muscles. In Caffeine-exposed muscles the Ca^{2+}-waves did not propagate into the jet region. This precluded determination of the site of origin of Ca^{2+}-waves, but the earliest Ca^{2+}-surge was also observed in the BZ. These observations suggest strongly that the Ca^{2+} surge in the BZ was the initiating event of Ca^{2+}-waves. The delay between peak of the last stimulated Ca^{2+}-transient and the start of the propagating Ca^{2+}-transient in the BZ decreased inversely with the amplitude of the initial Ca^{2+}-surge in all jet exposures.

3.4. Propagation of Ca^{2+}-waves

Propagation velocity of the Ca^{2+}-waves as in Fig. 3 outside and inside the jet region, ranged from 0.2 to 2.8 mm/s, i.e. comparable to Ca^{2+}-waves observed in studies of damaged muscle (Miura et al., 1998; Wakayama et al., 2001; Wakayama et al., 2005). V_{prop} correlated with the $[Ca^{2+}]_i$ increase seen in the BZ during the Ca^{2+}-surge. Furthermore, V_{prop} correlated with the amplitude of the waves both inside and outside the jet (Miura et al., 1999)(Fig. 3C). Propagation into the normal region occurred often with a gradual decline in amplitude. Only the fast waves propagated (1.6 ± 0.3 mm/s) into the normal region outside the jet with a negligible decrease in amplitude. Small waves propagated at lower V_{prop} and with decrement ($V_{prop} = 0.8\pm0.1$ mm/s), but completely through the region of observation ($\approx 450\,\mu m$). The slowest waves ($V_{prop} = 0.5\pm0.1$ mm/s) stopped after 200–300 μm. Frequently, waves propagating inside the jet region collided with the wave arriving from the opposite BZ and then terminated (see Fig. 3C).

3.5. Non-uniformity and arrhythmias

Whenever TPCs occur in muscles rendered non-uniform by damage, depolarizations accompany them similar to DADs with a duration that correlated exactly with the time during which the TPCs travel through the trabeculae; the amplitude of the DADs also correlated exactly with the amplitude of the TPCs (Daniels et al., 1991b). This tight correspondence between TPCs and DADs suggests that the DAD is elicited by a Ca^{2+}-dependent current as has been proposed by Kass and Tsien (Kass et al., 1978). Hence, if the $[Ca^{2+}]_i$ transient is large enough it is expected to lead to action potential formation. Clearly, non-uniformity due to damage initiates a chain of subcellular events leading to arrhythmogenic oscillations of $[Ca^{2+}]_i$ (Fig. 4A).

Experiments with muscles rendered non-uniform by a jet of solution containing an inhibitor of ECC prove that mechanical non-uniformity is a sufficient requirement for arrhythmogenicity. Fig. 4B shows that non-uniformity of ECC created by the jet induced rapidly reversible non-driven rhythmic activity. The arrhythmia consisted of spontaneous twitches at regular intervals starting after an after-contraction that followed the last stimulated contraction. The arrhythmia (muscle exposed to BDM) continued until the next stimulus train (7.5 s; Fig. 6B). The intervals between non-driven contractions were usually slightly longer than those of the preceding stimulus train. As shown in Fig. 4B, these arrhythmias were no longer inducible shortly after the jet was turned off and the uniformity of ECC restored.
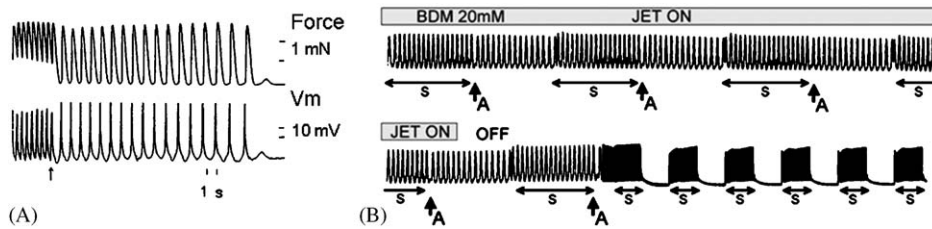
Fig. 4. Triggered propagated contractions cause arrhythmias. (A) Force (top tracing) and membrane potential (bottom tracing)recordings during a train of conditioning stimuli (ending at the arrow) and a subsequent triggered arrhythmia in muscle with a damaged end. Note the initial slow upstroke in both force and membrane potential of triggered twitches, suggestive of an underlying TPC and DAD. The triggered arrhythmia terminated spontaneously with an increase in the interval between triggered beats, followed by a TPC and DAD; $[Ca^{2+}]_o$ 2.25 mM. Resting membrane potential -71 mV. Modified from (Daniels, 1991). (B) Non-uniform ECC caused by the jet containing BDM (20 mmol/L) is arrhythmogenic. Recording of force showing that stimulus trains during local exposure to BDM (gray bars above the tracings) consistently induced arrhythmias(A). An expanded force tracing showing that spontaneous contractions were both preceded and followed by after-contractions induced by the stimulus train. OFF (arrow) indicates when the jet was turned off; this rapidly eliminated the contractile non-uniformity and its arrhythmogenic effects. S indicates stimulus trains (2.5 Hz—7.5 s) repeated every 15 s; during the last six trains the chart speed was reduced 2.5 fold. $[Ca^{2+}]_o = 3.5$ mmol/L; temperature 25.8 °C.

3.6. Simulation of ECC with feedback between force and Ca^{2+} dissociation from TnC

We have tested whether feedback of the force to TnC Ca^{2+} kinetics (Landesberg and Sideman, 1994b) reproduces the Ca^{2+} surge that appears to trigger the Ca^{2+}-waves. In order to test the general applicability of the model we have first studied whether the model reproduces the characteristic features of cardiac muscle in the steady state and during the twitch. For the twitch we have simplified the model compared to existing models to a single release pulse and we have simplified the relaxation phase by assuming a single Ca^{2+} removal process. These assumptions generated the time course of $[Ca^{2+}]_i$ similar to that of unloaded cardiac myocytes (Michailova et al., 2002). Intracellular Ca^{2+} was assumed to bind to intracellular ligands including TnC, and ATP. Ca^{2+} was assumed to bind to a single low affinity site on TnC with a fixed on rate constant, but to dissociate with an off-rate that was inversely proportional to the Ca · TnC deformation caused by XB-force that strains the actin filament (κ). The rate of formation (f) of force developing cross bridges was fit to the rate of force development of trabeculae after a quick release but ratio of f and g was taken from the literature (Woledge et al., 1985).

Fig. 5 shows that simulation of the feedback of F to Ca^{2+} dissociation from Ca^{2+}TnC through deformation of the actin filament and TnC on the filament by a single feedback of actin strain κ predicts fundamental properties known for cardiac muscle. The first is a realistic reproduction of the steady state F–pCa relationship which is known from experiments at controlled SL (Kentish et al., 1986b). Fig. 5A shows that an increase of SL causes an apparent shift of the F–pCa relationship to lower pCa when the muscle is stretched as a result of an increase of the apparent Hill coefficient (or steepness of the curves), although TnC still is assumed to bind only one Ca^{2+} ion. It is not surprising that the feedback predicts realistic F–SL relationships at varied activation levels for $[Ca^{2+}]_i$ (Fig. 5B).
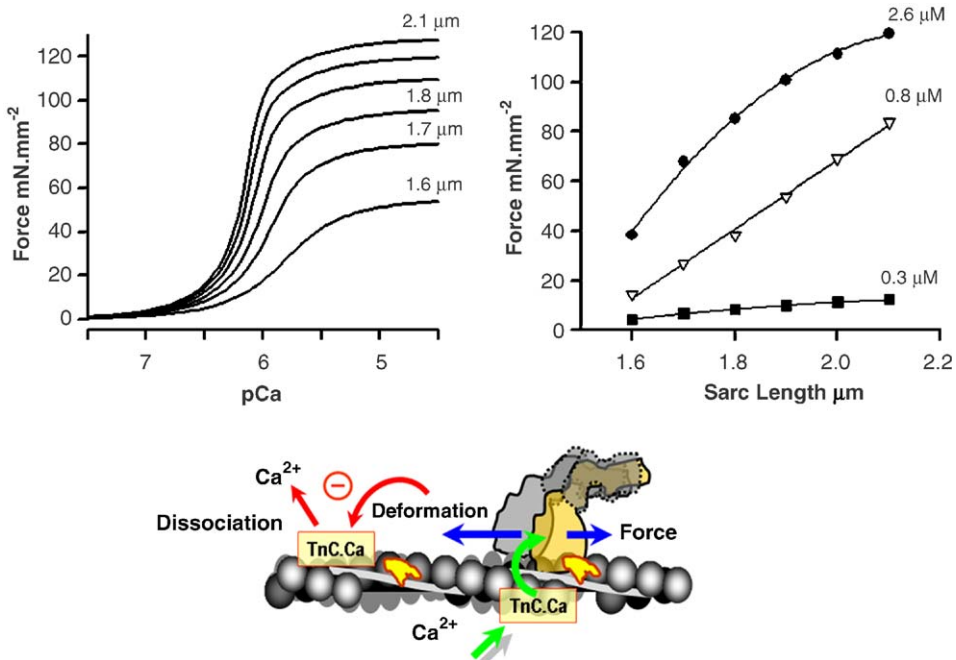
Fig. 5. Center panel shows a cartoon of the cross bridge- actin–TnC interaction. We assume in the model that that force development by XBs feeds back on dissociation of Ca^{2+} ions from $Ca \cdot TnC$ by inducing a deformation of $Ca \cdot TnC$ complex, which reduces the off-rate of Ca^{2+} from Ca^{2+}.Tnc. Left top shows the F–pCa curves which result from this feedback ($\kappa = 0.025$). These curves are identical to the measured F–pCa curves(Kentish et al., 1986b). Right top: The F–SL curves at three levels of $[Ca^{2+}]_i$ are also near-identical to the published F–SL both in skinned trabeculae and in intact cardiac trabeculae (Kentish et al., 1986b).

Increased force development increases the duration of Ca^{2+} binding to TnC and hence the duration of the twitch. Such a progressive prolongation of the twitch has indeed been shown for cardiac muscle twitches at constant sarcomere length and is reproduced accurately by the introduction of a tight relationship between the actin strain κ and a decrease of the dissociation rate of Ca from $Ca^{2+}TnC$ (Landesberg and Sideman, 1994b; ter Keurs et al., 1980a). This observation holds both in model and experiments irrespective whether the increased force is caused by varied SL, or $[Ca^{2+}]_o$ or by other interventions (Bucx, 1995). Fig. 6 shows that twitch prolongation is accompanied by a proportional prolongation of the time during which TnC is occupied by Ca^{2+} ions (Fig. 6, left bottom). Conversely, any force-decrease is expected to cause accelerate dissociation of Ca from $Ca^{2+}TnC$ and to decrease to subsequent force. This phenomenon is the well known as the deactivation response to shortening and is realistically replicated by the model (Fig. 6). The degree of force reduction during shortening de-activation depends on the redistribution of Ca^{2+} over ligands and Ca^{2+} extrusion.

Fig. 7 also shows that the model reproduces our observation (Backx and ter Keurs, 1993) and the recent observation by Julian's group, that the $[Ca^{2+}]_i$ transient during the twitch exhibits a prominent plateau at higher force levels (Jiang et al., 2004). These authors explained their observation on the basis of cooperativity between force development and affinity of TnC for Ca^{2+} ions, but we are not aware of previous quantitative modeling explaining this observation. This
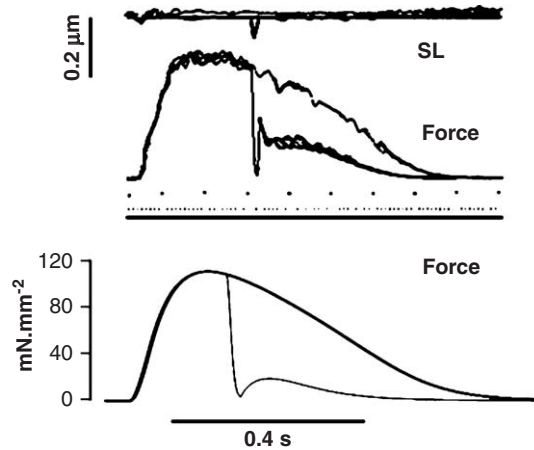
Fig. 6. Bottom panel shows the simulated time course of F during a twitch in the presence of feedback of F to the off-rate of Ca^{2+} from $Ca \cdot TnC$ ($\kappa = 0.025$). Both the time course of F and the effect of a quick release are identical to the effect of an experimental quick release during a twitch (shown in the top panel) that starts at constant sarcomere length of 2.15 μm (top-trace) in which a quick release of F is induced by a 30 ms lasting shortening transient 0.1 μm (ter Keurs et al., 1980a).

plateau is remarkable in the model as well, although the $[Ca^{2+}]_i$ transient in (Fig. 7) does not last longer than the force transient in contrast to the observed experimental fluorescence transient of Fura-2 (Backx and ter Keurs, 1993; Jiang et al., 2004). The plateau is completely lost in the absence of the feedback (Fig. 7).

Lastly, Fig. 7 shows the possible importance of this mechanism the response of F and $[Ca^{2+}]_i$ to a quick reduction of force in that the model predicts large $[Ca^{2+}]_i$ transients upon a quick release owing to Ca^{2+} dissociation from the $Ca^{2+}TnC$. The Ca^{2+} transient is well above the $[Ca^{2+}]_i$ level that is required to induce propagating CICR (Stuyvers et al., 2005). We postulate that these $[Ca^{2+}]_i$ transients occur in non-uniform muscle and cause reverse excitation–contraction coupling, which is responsible for Ca^{2+} waves TPCs , DADs and arrhythmias.

4. Discussion

4.1. Experimental non-uniform ECC

We have used in this study a novel model of non-uniform ECC in cardiac muscle to study the initiation of arrhythmogenic Ca^{2+}-waves underlying TPCs in cardiac muscle. We created non-uniformity in ECC by exposing a small segment of the muscle to Caffeine, BDM or Low $[Ca^{2+}]_o$. We expected that (1) Low-$[Ca^{2+}]_{jet}$ would reduce Ca^{2+}-currents and thereby SR-Ca^{2+} content (Bers, 2001), (2) Caffeine would open SR-Ca^{2+} release channels and thereby deplete the SR (Bers, 2001; Konishi et al., 1984; Kurihara and Komukai, 1995; Sitsapesan and Williams, 1990), and (3) BDM would modestly affect Ca^{2+}-transport(Backx et al., 1994; Herrmann et al., 1992; Sellin and McArdle, 1994) and inhibit cross-bridge cycling (Backx et al., 1994; Herrmann et al., 1992). Consistent with these expectations, the amplitude of stimulated Ca^{2+}-transients, which reflects
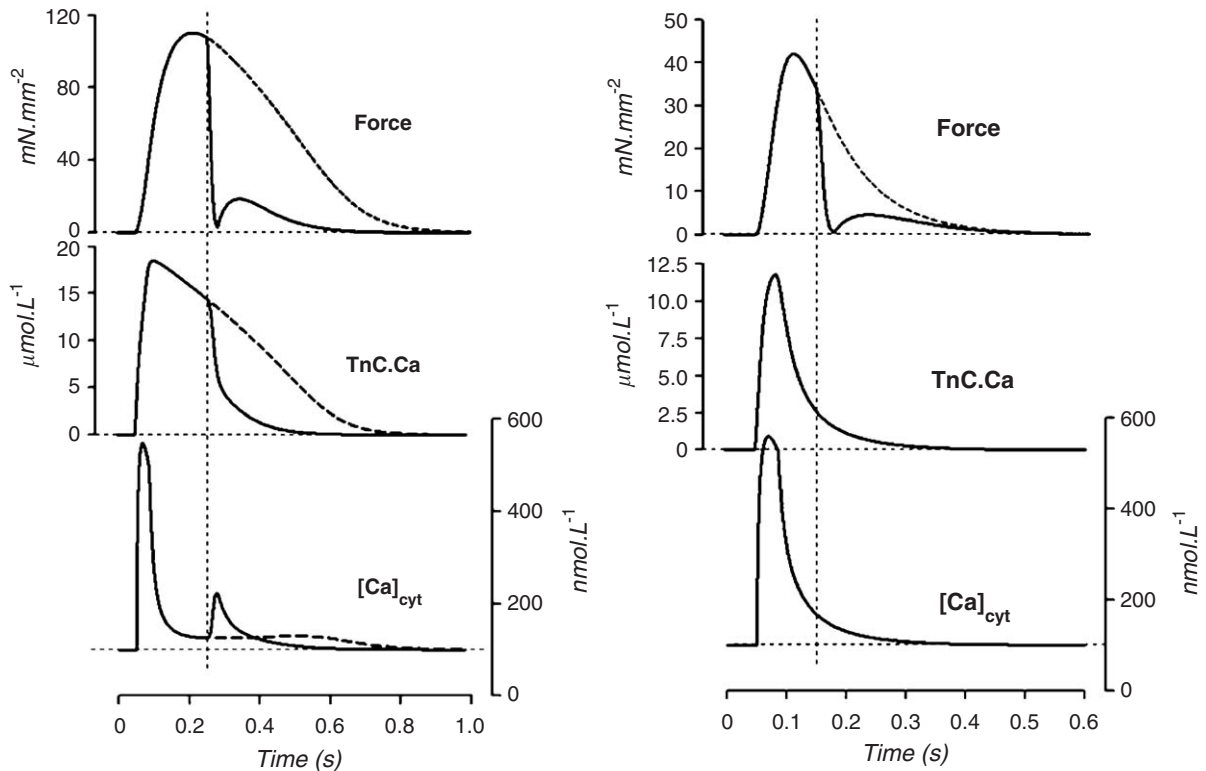
Fig. 7. The Left panel shows the simulated time course of F, free $[Ca^{2+}]_i$ and $[Ca \cdot TnC]$ during a twitch in the presence of feedback of F to the off-rate of Ca^{2+} from $Ca \cdot TnC$ ($\kappa = 0.025$). The time course of F is identical to the time course of F during the published sarcomere isometric contraction (van Heuningen et al., 1982). The time course of $[Ca^{2+}]_i$ is identical to the published time course of $[Ca^{2+}]_i$.(Jiang et al. 2004.) including the plateau of the $[Ca^{2+}]_i$ transient. The effect of feedback of F on dissociation of Ca^{2+} ions from $Ca \cdot TnC$ leads to prolonged binding of Ca^{2+} to TnC, which exceeds the time course of the $[Ca^{2+}]_i$ transient. The effect of a quick release of the muscle 200 ms after onset of contraction (indicated by the vertical dashed line through the tracings) causes a rapid drop of F and a rapid and large decrease of the amount of Ca^{2+} bound to $Ca \cdot TnC$, which causes a substantial increase in free $[Ca^{2+}]_i$, denoted here as the Ca^{2+} surge. The right panel shows the time course of F, free $[Ca^{2+}]_i$ and $[Ca \cdot TnC]$ during the twitch in the absence of feedback of F to the off-rate of Ca^{2+} from $Ca \cdot TnC$. Peak F is smaller and the $[Ca \cdot TnC]$now follows the $[Ca^{2+}]_i$ transient. A quick release (at the dashed line) still causes a rapid drop of force but fails to elicit a $[Ca^{2+}]_i$ transient during relaxation.

the SR-Ca^{2+} load (Bers, 2001), decreased dramatically in regions exposed to Caffeine and Low-$[Ca^{2+}]_{jet}$, but only slightly with BDM (Fig. 3). The effects of BDM are emphasized here because the drug quite apparently only reduced force development—at this concentration—in the jet-exposed region significantly and left the Ca^{2+} transients relatively unaffected.

Each of these perturbations reduced muscle force due to creation of a muscle segment, which developed less twitch force than the normal cells remote from the jet, as is witnessed by stretch of the weakened sarcomeres in the jet by the fully activated sarcomeres outside the exposed region. These regions were connected mechanically by a border zone, BZ of one to two cells, where the sarcomeres first contracted and, then, were stretched. The diffraction pattern of sarcomeres in the

BZ showed a clear single peak during both shortening and lengthening, strongly suggesting that sarcomere contraction in the BZ was also partially suppressed, probably owing to diffusion of the contents of each jet solution.

4.2. Non-uniform ECC and the Ca^{2+} surge

Ca^{2+}-waves and TPCs have been closely related to Ca^{2+}-overload in damaged regions and the resultant non-uniformity of muscle contraction (ter Keurs et al., 1998). However, in that model it is difficult to investigate the underlying mechanisms since damage is difficult to control. This study shows clearly that Ca^{2+}-waves are reversibly initiated in regions without damage and, more specifically, from the 'Border Zone', in which contraction is partially suppressed. The common effect of the three protocols was to suppress contraction and reduce sarcomere force; the latter occurred *with* (Caffeine, and Low $[Ca^{2+}]_{jet}$) or *without* change of the Ca^{2+} transient (BDM), and *with* (Caffeine) or *without* change of diastolic $[Ca^{2+}]_i$ (BDM). The observation that the effect of force was common to all three interventions while the effect on $[Ca^{2+}]_i$ and on the Ca^{2+}-transient was dramatically different between the interventions makes it reasonable to conclude that Ca^{2+}-waves are initiated as a result of non-uniformity of sarcomere force generation and the resultant sequence of stretch and release of sarcomeres in the BZ by contraction of normal cells in the region remote from the jet.

By varying $[Ca^{2+}]_o$ we detected a small localized $[Ca^{2+}]_i$ surge in the BZ, which developed into a propagating wave when $[Ca^{2+}]_o$ was increased (Fig. 3C). Once initiated, these Ca^{2+}-waves traveled from the region with the localized $[Ca^{2+}]_i$ rise proving that this region constitutes the initiation site for Ca^{2+}-waves.

The initiating Ca^{2+}-surge took place late during the relaxation phase of the twitch when both force and free Ca^{2+} in the cytosol had decayed by 70–80% (Fig. 3D). By this time the SR-Ca^{2+} channels have partially recovered (Banijamali et al., 1998) and are able to support CICR and Ca^{2+} wave generation (Bers, 2001). However, the delay between the start of the stimulus and the Ca^{2+}-surge makes it highly unlikely that Ca^{2+}-entry via L-type Ca^{2+}-channels causes CICR from the SR involved in the initial Ca^{2+} surge. Furthermore, Ca^{2+}-waves never started in jet-exposed regions where sarcomeres were maximally stretched even if the amplitude of the stimulated Ca^{2+}-transients witnessed a robust SR-Ca^{2+} load (Bers, 2001). Ca^{2+}-waves never started simultaneously with the peak of the stretch (Fig. 4C) making it unlikely that a stretch-related mechanism such as activation of Gd^{3+}-sensitive stretch-activated channels (Backx and ter Keurs, 1993; ter Keurs et al., 1980b; Wakayama et al., 2001; Zhang et al., 1996; Zhang and ter Keurs, 1996) is involved in the initial Ca^{2+}-surge. Finally, Ca^{2+}-waves started from the BZ with reduced SR-Ca^{2+}-release (CF and Low-$[Ca^{2+}]_{jet}$) and/or reduced $[Ca^{2+}]_i$ (Low-$[Ca^{2+}]_{jet}$ and BDM), suggests to us that another mechanism of wave initiation different from "spontaneous SR Ca^{2+}-release" was involved.

4.3. Initiation and propagation of Ca^{2+}-waves

We propose an alternative explanation on the basis of these experiments and the results of model studies. It is likely that quick-release-induced Ca^{2+}-dissociation from the myofilaments, demonstrated in uniform cardiac muscle, is applicable to the chain of cells in the non-uniform

muscle exposed to the jet. Rapid sarcomere shortening during the force decline occurred both in the jet region and in the BZ, but led only to a Ca^{2+} surge and Ca^{2+}-wave initiation in the BZ (Fig. 3C), making it probable that quick-release-induced Ca^{2+}-dissociation from TnC caused by the decline of force in the shortening BZ sarcomeres led to the local Ca^{2+} surge (Allen and Kentish, 1988b; Allen and Kurihara, 1982; Backx and ter Keurs, 1993; Housmans et al., 1983; Kurihara and Komukai, 1995; Lab et al., 1984). The region inside the jet, where ECC was all-but abolished probably contained either little $TnC-Ca^{2+}$ (Caffeine or Low-$[Ca^{2+}]_{jet}$) or only few Ca^{2+}-activated force-generating cross-bridges (BDM), which would render a quick release of this region unable to generate a Ca^{2+}-surge and Ca^{2+}-wave . The BZ, on the other hand, could generate a Ca^{2+}-surge that is large enough to induce local CICR and thus a Ca^{2+}-wave even if only a fraction of TnC (Backx et al., 1989; Fabiato, 1983) were occupied with Ca^{2+} (ter Keurs et al., 1998).

A precise quantitative analysis of the relation between quick release dynamics and onset of the Ca^{2+}-surge and/or waves may shed further light on this mechanism of initiation of Ca^{2+}-waves. Our present study allows for an estimate of the latency ($\sim$40 ms) between rapid F and SL changes and the initial rise of $[Ca^{2+}]_i$ during the Ca^{2+}-surge in a small BZ region $\sim$100 μm (Fig. 3D). Cannell and Allen have shown that it requires $\approx$20 ms for an intra-sarcomeric ($\approx$1 μm) Ca^{2+}-gradient to dissipate (Cannell and Allen, 1984). Hence, the minimum value for the delay between Ca^{2+}-dissociation of the filaments and $SR-Ca^{2+}$-release could correspond to Ca^{2+} diffusion from the myofilaments to $SR-Ca^{2+}$ release sites over at most a few sarcomere lengths.

Ca^{2+}-waves propagated in this model at slightly lower velocity (0.2–2.8 mm/s) than those of previous studies of regionally damaged muscles (Miura et al., 1998; Raisaro et al., 1993; Wakayama et al., 2001). In this study the amplification of the Ca^{2+}-signal by $SR-Ca^{2+}$-release required for propagation may have been lower in the absence of Ca^{2+}-loading of the muscle by damaged areas (Daniels and ter Keurs, 1990; Mulder et al., 1989; Backx et al., 1989; Kaneko et al., 2000; Lamont et al., 1998; Miura et al., 1999; ter Keurs et al., 1998; Wier et al., 1997; Zhang et al., 1996). A lower cellular Ca^{2+}-load would explain the occurrence of smaller Ca^{2+}-waves that propagated both more slowly and with a gradual decline of their amplitude and disappeared after a few hundred metres. Ca^{2+}-waves did propagate into the region with normal $SR-Ca^{2+}$-release such as inside the BDM jet (Fig. 3D) and propagated slowly inside the Low-$[Ca^{2+}]$ jet where the $SR-Ca^{2+}$-load is expected to be reduced. Ca^{2+}-waves did not propagate through the region exposed to Caffeine (data not shown), which is consistent with the effect of Caffeine to deplete $SR-Ca^{2+}$ required for wave propagation (Miura et al., 1999).

4.4. Feedback between cross-bridge force and Ca^{2+} dissociation from TnC

Fig. 4 shows the fundamental property of Xb–TnC interaction that underlies the model: feedback of F to Ca^{2+} dissociation from Ca^{2+}TnC through the strain **κ** of the actin filament and subsequent deformation of TnC on the filament predicts fundamental properties known for cardiac muscle. In view of the realistic reproduction of the steady-state F–pCa relationship (Fig. 5) (Kentish et al., 1986a), is it not surprising that the feedback predicts realistic F–SL relationships at varied activation levels for $[Ca^{2+}]_i$. The prediction by the model that the F–SL exhibits little sensitivity to shortening, as has been observed (ter Keurs et al., 1980b) needs to be

tested in order to ascertain its merit in explaining both the end-systolic pressure volume relationship (ESPVR) described by Suga an Sagawa and Starling's Law of the heart .

Twitches generated by the model are similar to twitches generated by rat cardiac trabeculae at 25 °C. The increased time of Ca^{2+}-binding to TnC as a result of the feedback of force development explains progressive prologation of the twitch has indeed been shown for cardiac muscle twitches at varied length, while SL was held constant during the twitch (ter Keurs et al., 1980a). This property was reproduced accurately by introducing a close relationship between the actin strain κ and a decrease of the dissociation rate of Ca from Ca^{2+}TnC. This observation holds both in model and experiments irrespective whether the increased force is caused by varied SL, or $[Ca^{2+}]_o$ or varied pH (Bucx, 1995). Conversely, any force-decrease is expected to cause accelerate dissociation of Ca^{2+} from Ca^{2+}TnC and to decrease to subsequent force. This phenomenon is the well known as the deactivation response to shortening and is realistically replicated by the model (Fig. 6). The degree of force reduction during shortening de-activation depends on the redistribution of Ca^{2+} over ligands and Ca^{2+} extrusion.

The simulations also reproduced our observation (Backx and ter Keurs, 1993) and the recent observation by Julian's group, that the $[Ca^{2+}]_i$ transient during the twitch exhibits a prominent plateau at higher force levels (Jiang et al., 2004). The latter authors explained their observation on the basis of cooperativity between force development and affinity of TnC for Ca^{2+} ions, but we are not aware of previous quantitative modeling explaining this observation. The plateau is obvious in the $[Ca^{2+}]_i$ simulation of Fig. 7 (left panel) as well, and is completely lost in the absence of the feedback (Fig. 7). The observation that the simulated $[Ca^{2+}]_i$ transient does not last longer than the fluorescence transient in the two aforementioned studies (Backx and ter Keurs, 1993; Jiang et al., 2004). The predicted fluorescent transients in our simulations (data not shown) were similar to those measured experimentally; the difference in time course was explained by the limited dissociation rate of Ca^{2+} from Fura-2 (80–130 $\mu M^{-1} s^{-1}$) (Backx and ter Keurs, 1993; Jiang et al., 2002; Kao and Tsien, 1988). The combination of these predictions is no proof for the postulated Force–Ca^{2+}TnC feedback, but makes it a useful working model for cardiac muscle and should stimulate further studies of the dynamics of the interaction between TnC and Ca^{2+}.

4.5. Implication: non-uniform ECC, Ca^{2+}-waves and arrhythmias

In this study of controlled non-uniformity of muscle contraction, we identify non-uniform contraction in cardiac muscle for the first time as a possible arrhythmogenic mechanism owing to a Ca^{2+}-surge that results from Ca^{2+} dissociation from Ca^{2+}TnC during relaxation. Simulations using a model, which assumes that XB force retards Ca^{2+} dissociation from the $Ca \cdot TnC$ complex on actin, indeed, predict a large $[Ca^{2+}]_i$ transient upon a quick release owing to Ca^{2+} dissociation from the Ca^{2+}TnC. The Ca^{2+} transient is well above the $[Ca^{2+}]_i$ level that is required to induce propagating CICR (Stuyvers et al., 2005). We postulate that these $[Ca^{2+}]_i$ transients occur in non-uniform muscle and cause reverse excitation–contraction coupling (Fig. 2), which is responsible for Ca^{2+}-waves TPCs , DADs and arrhythmias. Such Ca^{2+} waves are known to cause transient depolarizations (Daniels et al., 1991b; Lakatta, 1992; Miura et al., 1993; Schlotthauer and Bers, 2000; Wakayama et al., 2001) and cause arrhythmias (Daniels et al., 1991b) (Fig. 4).

Whether this mechanism contributes to arrhythmias in diseased heart where non-uniform segmental wall motion (Siogas et al., 1998; Young et al., 2001) may result from

ischemia, non-uniform electrical activation or non-uniform adrenergic activation (Jiang and Julian, 1997; Siogas et al., 1998) remains to be proven, although the arrangement of the cardiac wall in muscle fascicles, which transmit force longitudinally and therefore are subject to comparable constraints as the trabeculae in this study makes this possibility likely high. Importantly, our model of RECC also predicts that the initial Ca^{2+}-surge from TnC will lead more readily to arrhythmias in hearts with abnormal SR-Ca^{2+} storage (Laitinen et al., 2001; Marks, 2001; Postma et al., 2002) and/or with increased open probability of the SR-Ca^{2+}-release channels (Boyden and ter Keurs, 2001) owing to either mutation of the channel gene (Laitinen et al., 2001; Schlotthauer and Bers, 2000; Siogas et al., 1998) or to post-translational changes of the channel in heart failure (Marks, 2001).

Acknowledgements

Editor's note

For all related communications in this volume see Cens et al. (2005) and Hinch et al. (2005). For further information and downloadable content please see http://www.physiome.org.nz/publications/PBMB-2005-89/TerKeurs/

Appendix A. Parameters, variables and units

T	Time (s)
t_s	Start time (s)
A	Magnitude of Ca^{2+}-release (mol/L)
τ_{on}	On-time constant (s)
τ_{off}	Off-time constant (s)
$[Ca]_{Rest}$	Resting $[Ca^{2+}]$ (nmol/L)
$[Ca]_t$	Instantaneous $[Ca^{2+}]$ (nmol/L)
R	Ca^{2+}-release flux (number of Ca^{2+} ions/s)
U	Ca^{2+}-uptake flux (number of Ca^{2+} ions/s)
U_{MAX}	Maximal Ca^{2+}-uptake flux (number of Ca^{2+} ions/s)
EC_{U50}	Ca^{2+} at half maximal uptake (nmol/L)
f and g	Rate of attachment and detachment of XBs
$k_+^{ATP}, k_+^{TnC}, k_+^{Fluo4}$	Ca^{2+} on-rate constants for ATP, TnC and Fluo-4.
$k_-^{ATP}, k_-^{TnC}, k_-^{Fluo4}$	Ca^{2+} off-rate constants for ATP, TnC and Fluo-4 .
[ATP], [TnC],[Fluo4], [Myosin]	ATP, TnC, Fluo-4 and Myosin concentrations (nmol/L)
[CaATP],[Ca·TnC], [CaFluo4]	Ca^{2+}–ATP, Ca^{2+}–TnC, Ca^{2+}–Fluo4 concentrations (nmol/L)

References

Allen, D.G., Kentish, J.C., 1985. The cellular basis of the length–tension relation in cardiac muscle. J.Mol. Cell. Cardiol. 17, 821–840.

Allen, D.G., Kentish, J.C., 1988a. Calcium concentration in the myoplasm of skinned ferret ventricular muscle following changes in muscle length. J. Physiol. 407, 489–503.

Allen, D.G., Kentish, J.C., 1988b. Calcium concentration in the myoplasm of skinned ferret ventricular muscle following changes in muscle length. J. Physiol. 407, 489–503.

Allen, D.G., Kurihara, S., 1982. The effects of muscle length on intracellular calcium transients in mammalian cardiac muscle. J. Physiol. 327, 79–94.

Backx, P.H., ter Keurs, H.E.D.J., 1993. Fluorescent properties of rat cardiac trabeculae microinjected with fura-2 salt. Am. J. Physiol. 264, H1098–H1110.

Backx, P.H.M., de Tombe, P.P., van Deen, J.H.K., Mulder, B.J.M., ter Keurs, H.E.D.J., 1989. A model of propagating calcium-induced calcium release mediated by calcium diffusion. J. Gen. Physiol. 93, 963–977.

Backx, P.H., Gao, W.D., Azan-Backx, M.D., Marban, E., 1994. Mechanism of force inhibition by 2,3-butanedione monoxime in rat cardiac muscle: roles of $[Ca^{2+}]i$ and cross-bridge kinetics. J. Physiol. 476, 487–500.

Backx, P.H.M., Gao, W.D., Azan-Backx, M.D., Marban, E., 1995. The relationship between contractile force and intracellular $[Ca++]$ in intact rat cardiac trabeculae. J. Gen. Physiol. 105, 1–19.

Banijamali, H.S., Gao, W.D., MacIntosh, B.R., ter Keurs, H.E.D.J., 1991. Force–interval relations of twitches and cold contractures in rat cardiac trabeculae: influence of ryanodine. Circ. Res. 69, 937–948.

Banijamali, H., Gao, W.D., MacIntosh, B., ter Keurs, H.E.D.J., 1998. Force–interval relations of twitches and cold contractures in Rat cardiac trabeculae; effect of Ryanodine. Circ. Res. 69, 937–948.

Bers, D.M., 2001. Excitation Contraction Coupling and Cardiac Contractile Force, second ed. Kluwer Academic Publishers, Dordrecht, Boston, London.

Boyden, P.A., ter Keurs, H.E.D.J., 2001. Reverse excitation contraction coupling: Ca^{2+} ions as initiators of arrhythmias. J. Cardiovasc. Electrophysiol. 12, 382–385.

Bucx, J.J.J., 1995. Ischemia of the heart: a study of sarcomere dynamics and cellular metabolism. Ph.D. Thesis.

Cannell, M.B., Allen, D.G., 1984. Model of calcium movements during activation in the sarcomere of frog skeletal muscle. Biophys. J. 45, 913–925.

Cens, T., Rousset, M., Leyris, J.-P., et al., 2005. Voltage and calcium-dependent inactivation in high voltage-gated Ca^{2+} channels. Prog. Biophys. Mol. Biol. 89.

Cranefield, P.F., 1977. Action potentials, afterpotentials, and arrhythmias. Circ. Res. 41, 415–423.

Csernoch, L., Zhou, J., Stern, M.D., Brum, G., Rios, E., 2004. The elementary events of Ca^{2+} release elicited by membrane depolarization in mammalian muscle. J. Physiol. 557, 43–58.

Daniels, M.C.G., ter Keurs, H.E.D.J., 1990. Spontaneous contractions in rat cardiac trabeculae; trigger mechanism and propagation velocity. J. Gen. Physiol. 95, 1123–1137.

Daniels, M.C.G., 1991. Mechanism of triggered arrhythmias in damaged myocardium. Ph.D.Thesis.

Daniels, M.C.G., Fedida, D., Lamont, C., ter Keurs, H.E.D.J., 1991a. Role of the sarcolemma in triggered propagated contractions in rat cardiac trabeculae. Circ. Res. 68, 1408–1421.

Daniels, M.C.G., Fedida, D., Lamont, C., ter Keurs, H.E.D.J., 1991b. Role of the sarcolemma in triggered propagated contractions in rat cardiac trabeculae. Circ. Res. 68, 1408–1421.

Davidoff, A.W., Boyden, P.A., Schwartz, K., Michel, J.B., Zhang, Y.M., Obayashi, M., Crabbe, D., ter Keurs, H.E., 2004. Congestive heart failure after myocardial infarction in the rat: cardiac force and spontaneous sarcomere activity. Ann. N.Y. Acad. Sci. 1015, 84–95.

Fabiato, A., 1983. Calcium-induced release of calcium from the cardiac sarcoplasmic reticulum. Am. J. Physiol. 245, C1–C14.

Ferrier, G.R., 1976. The effects of tension on acetylstrophanthidin-induced transient depolarizations and after-contractions in canine myocardial and Purkinje tissues. Circ. Res. 38, 156–162.

Herrmann, C., Wray, J., Travers, F., Barman, T., 1992. Effect of 2,3-butanedione monoxime on sarcoplasmic reticulum of saponin-treated rat cardiac muscle. Biochemistry 31, 12227–12232.

Hinch, R., Greenstein, J.L., Winslow, R.L., 2005. Multi-scale models of local control of calcium induced calcium release. Prog. Biophys. Mol. Biol. 89.

Housmans, P.R., Lee, N.K.M., Blinks, J.R., 1983. Active shortening retards the decline of the intracellular calcium transient in mammalian heart muscle. Science 221, 159–161.

Ishide, N., Miura, M., Sakurai, M., Takishima, T., 1992. Initiation and development of calcium waves in rat myocytes. Am. J. Physiol. 263, H327–H332.

Jiang, Y., Julian, F.J., 1997. Pacing rate, halothane, and BDM affect fura 2 reporting of $[Ca^{2+}]_i$ in intact rat trabeculae. Am. J. Physiol. 273, C2046–C2056.

Jiang, D., Xiao, B., Zhang, L., Chen, W., 2002. Enhanced basal activity of a cardiac Ca^{2+} release channel (ryanodine receptor) mutant associated with ventricualr tachycardia and sudden death. Circ. Res. 91, 218–225.

Jiang, Y., Patterson, M.F., Morgan, D.L., Julian, F.J., 2004. Basis for late rise in fura 2 R signal reporting $[Ca^{2+}]_i$ during relaxation in intact rat ventricular trabeculae. Am. Physiol. Soc. 43, C1273–C1282.

Kaneko, T., Tanaka, H., Oyamada, M., Kawata, S., Takamatsu, T., 2000. Three distinct types of Ca^{2+} waves in Langendorff-perfused rat heart revealed by real-time confocal microscopy. Circ. Res. 86, 1093–1099.

Kao, J.P., Tsien, R.Y., 1988. Ca^{2+} binding kinetics of fura-2 and azo-1 from temperature-jump relaxation measurements. Biophys. J. 53, 635–639.

Kass, R.S., Lederer, W.J., Tsien, R.W., Weingart, R., 1978. Role of calcium ions in transient inward currents and aftercontractions induced by strophanthidin in cardiac purkinje fibres. J. Physiol. 281, 187–208.

Kentish, J.C., ter Keurs, H.E.D.J., Ricciardi, L., Bucx, J.J.J., Noble, M.I.M., 1986a. Comparison between the sarcomere length-force relations of intact and skinned trabeculae from rat right ventricle. Circ. Res. 58, 755–768.

Kentish, J.C., ter Keurs, H.E.D.J., Ricciardi, L., Bucx, J.J.J., Noble, M.I.M., 1986b. Comparison between the sarcomere length-force relations of intact and skinned trabeculae from rat right ventricle. Circ. Res. 58, 755–768.

Konishi, M., Kurihara, S., Sakai, T., 1984. The effects of caffeine on tension development and intracellular calcium transients in rat ventricular muscle. J. Physiol. 355, 605–618.

Kort, A.A., Lakatta, E.G., 1984. Calcium-dependent mechanical oscillations occur spontaneously in unstimulated mammalian cardiac tissues. Circ. Res. 54, 396–404.

Kurihara, S., Komukai, K., 1995. Tension-dependent changes of the intracellular Ca^{2+} transients in ferret ventricular muscles. J. Physiol. 489, 617–625.

Lab, M.J., Allen, D.G., Orchard, C.H., 1984. The effects of shortening on myoplasmic calcium concentration and on the action potential in mammalian ventricular muscle. Circ. Res. 55, 825–829.

Laitinen, P.J., Brown, K.M., Piippo, K., Swan, H., Devaney, J.M., Brahmbhatt, B., Donarum, E.A., Marino, M., Tiso, N., Viitasalo, M., Toivonen, L., Stephan, D.A., Kontula, K., 2001. Mutations of the cardiac ryanodine receptor (RyR2) gene in familial polymorphic ventricular tachycardia. Circulation 103, 485–490.

Lakatta, E.G., 1992. Functional implications of spontaneous sarcoplasmic reticulum Ca^{2+} release in the heart. Cardiovasc. Res. 26, 193–214.

Lamont, C., Luther, P.W., Balke, C.W., Wier, G.W., 1998. Intercellular Ca^{2+} waves in rat heart muscle. J. Physiol. 512, 669–676.

Landesberg, A., Sideman, S., 1994a. Coupling calcium binding to troponin-C and cross-bridge cycling in skinned cardiac cells. Am. J. Physiol. 266, H1260–H1271.

Landesberg, A., Sideman, S., 1994b. Mechanical regulation in the cardiac muscle by coupling calcium kinetics with crossbridge cycling; a dynamic model. Am. J. Physiol. 267, H779–H795.

Marks, A.R., 2001. Ryanodine receptors/calcium release channels in heart failure and sudden cardiac death. J. Mol. Cell. Cardiol. 33, 615–624.

Michailova, A., DelPrincipe, F., Egger, M., Niggli, E., 2002. Spatiotemporal features of Ca^{2+} buffering and diffusion in atrial cardiac myocytes with inhibited sarcoplasmic reticulum. Biophys. J. 83, 3134–3151.

Miura, M., Ishide, N., Oda, H., Sakurai, M., Shinozaki, T., Takishima, T., 1993. Spatial features of calcium transients during early and delayed afterdepolarizations. Am. J. Physiol. 265, H439–H444.

Miura, M., Boyden, P.A., ter Keurs, H.E.D.J., 1998. Ca^{2+} waves during triggered propagated contractions in intact trabeculae. Am. J. Physiol. 274, H266–H276.

Miura, M., Boyden, P.A., ter Keurs, H.E.D.J., 1999. Ca^{2+} waves during triggered propagated contractions in intact trabeculae; determinants of the velocity of propagation. Circ. Res. 84, 1459–1468.

Mulder, B.J.M., de Tombe, P.P., ter Keurs, H.E.D.J., 1989. Spontaneous and propagated contractions in rat cardiac trabeculae. J. Gen. Physiol. 93, 943–961.

Postma, A.V., Denjoy, I., Joorntje, T.M., Lupoglazoff, J-M., DaCosta, A., Sebillon, P., Mannens, M., Wilde, A.A.M., Guicheney, P., 2002. Absence of calsequesterin 2 causes severe forms of catecholaminergic polymorphic ventricular tachycardia. Circ. Res. 91, e21–e26.

Raisaro, A., Villa, A., Recusani, F., Rossi, A., Bargiggia, G., Tronconi, L., Campani, R., Montemartini, C., 1993. The remodelling of the heart in heart failure: from thoracic radiography to magnetic resonance. G. Ital. Cardiol. 23, 167–175.

Schlotthauer, K., Bers, D.M., 2000. Sarcoplasmic reticulum Ca(2 +) release causes myocyte depolarization. Underlying mechanism and threshold for triggered action potentials. Circ. Res. 87, 774–780.

Sellin, L.C., McArdle, J.J., 1994. Multiple effects of 2,3-butanedione monoxime. Pharmacol. Toxicol. 74, 305–313.

Siogas, K., Pappas, S., Graekas, G., Goudevenos, J., Liapi, G., Sideris, D.A., 1998. Segmental wall motion abnormalities alter vulnerability to ventricular ectopic beats associated with acute increases in aortic pressure in patients with underlying coronary artery disease. Heart 79, 268–273.

Sitsapesan, R., Williams, A.J., 1990. Mechanisms of caffeine activation of single calcium-release channels of sheep cardiac sarcoplasmic reticulum. J. Physiol. 423, 425–439.

Spooner, P.M., Rosen, M.R., 2001. Foundations of cardiac arrhythmias. Basic concepts and clinical approaches.

Stern, M.D., Kort, A.A., Bhatnagar, G.M., Lakatta, E.G., 1983. Scattered-light intensity fluctuations in diastolic rat cardiac muscle caused by spontaneous calcium-dependent cellular mechanical oscillations. J. Gen. Physiol. 82, 119–153.

Stuyvers, B., Miura, M., ter Keurs, H.E.D.J., 1997. Dynamics of viscoelastic properties of rat cardiac sacromeres during the diastolic interval: Involvement of Ca^{2+}. J. Physiol. 502, 661–667.

Stuyvers, B.D., Dun, W., Matkovich, S., Sorrentino, V., Boyden, P.A., ter Keurs, H.E.D.J., 2005. Ca^{2+} sparks and waves in Canine Purkinje Cells; a triple layered system of Ca^{2+} activation. Circ Res 97, 35–43.

ter Keurs, H.E.D.J., Rijnsburger, W.H., van Heuningen, R., 1980a. Restoring forces and relaxation of rat cardiac muscle. Eur. Heart J. 1 (suppl.A), 67–80.

ter Keurs, H.E.D.J., Rijnsburger, W.H., van Heuningen, R., Nagelsmit, M.J., 1980b. Tension development and sarcomere length in rat cardiac trabeculae. Evidence of length-dependent activation. Circ. Res. 46, 703–714.

ter Keurs, H.E.D.J., Zhang, Y.M., Miura, M., 1998. Damage induced arrhythmias: reversal of excitation-contraction coupling. Cardiovasc. Res. 40, 444–455.

ter Keurs, H.E.D.J., Hollander, E.H., ter Keurs, M.H.C., 2000. The effects of sarcomere length on the force-cytosolic Ca^{2+} relationship in intact rat trabeculae.

van Heuningen, R., Rijnsburger, W.H., ter Keurs, H.E.D.J., 1982. sarcomere length control in striated muscle. Am. J. Physiol. 242, H411–H420.

Wakayama, Y., Sugai, Y., Kagaya, Y., Watanabe, J., ter Keurs, H.E.D.J., 2001. Stretch and quick release of cardiac trabeculae accelerates Ca^{2+} waves and triggered propagated contractions. Am. J.Physiol. Circ. Physiol. 281, H2133–H2142.

Wakayama, Y., Miura, M., Stuyvers, B.D., Boyden, P.A., ter Keurs, H.E.D.J., 2005. Spatial non-uniformity of excitation-contraction coupling causes arrhythmogenic Ca^{2+} waves in rat cardiac muscle. Circ Res 96, 1266–1273.

Wier, W.G., ter Keurs, H.E.D.J., Marban, E., Gao, W.D., Balke, W., 1997. Ca^{2+} 'sparks' and waves in intact ventricular muscle resolved by confocal imaging. Circ. Res. 81, 462–469.

Woledge, R.C., Curtin, N.A., Homsher, E., 1985. Basic Facts and Ideas, pp. 1–26.

Young, A.A., Dokos, S., Powell, K.A., Sturm, B., McCulloch, A.D., Starling, R.C., McCarthy, P.M., White, R.D., 2001. Regional heterogeneity of function in nonischemic dilated cardiomyopathy. Cardiovasc. Res. 49, 308–318.

Zhang, Y., ter Keurs, H.E.D.J., 1994. Are stretch activated channels involved in triggered propagated contractions in rat cardiac trabeculae? Biophys. J. 66, A317.

Zhang, Y., ter Keurs, H.E.D.J., 1996. Effects of gadolinium on twitch force and triggered propagated contractions in rat cardiac trabeculae. Cardiovasc. Res. 32, 180–188.

Zhang, Y., Miura, M., ter Keurs, H.E.D.J., 1996. Triggered propagated contractions in rat cardiac trabeculae; inhibition by octanol and heptanol. Circ. Res. 79, 1077–1085.